Study of Structural and Magnetic Properties, Trivalent Cation Substitution of Cobalt base Spinel Ferrites $CoCr_{0.04}La_xFe_{1.96-x}O_4$ ($0 \leq x \leq 0.12$)

G. MUSTAFA
Department of Physics, Bahauddin, Zakariya University Multan, 60800, Pakistan
Z. FAROOQ
University of Education (Lahore) FSD
M.R. AHMAD
University Lahore
H. ANWAR
Department of Physics, University of Agriculture Faisalabad, 38040, Pakistan
H. AKHTAR
Department of Physics, University of Agriculture Faisalabad, 38040, Pakistan
M. YASEEN
University of Education
M. A. QAYYUM
University of Education
MIAN H.R. MAHMOOD (mianhrm01@yahoo.com)
University of Education

Research Article

Keywords: Nanoparticle, Co-precipitation Method, X-ray diffraction, M-H loop

Posted Date: July 1st, 2020

DOI: https://doi.org/10.21203/rs.3.rs-35369/v1

Abstract

In this research work a series of polycrystalline trivalent cation (Cr^{3+}, La^{3+}) substituted cobalt ferrite with general formula $CoCr_{0.04}La_xFe_{1.96-x}O_4$ where $0.00 \leq x \leq 0.12$ (in steps of 0.02) was synthesized using co-precipitation method and were sintered at 900°C for 6 hours. The phase identification and confirmation of the structure were confirmed employing the X-ray diffraction (XRD) and FTIR techniques. The size of crystallite was found on average, in the range of 53-106 nano-meters. FTIR results confirmed spinel ferrites structure. Moreover the morphological studies were observed through SEM. The elemental analysis of the samples was done by EDX while, I-V characterization of the represented sample was recorded using two probe method. The measured electrical resistivity of materials increased as dopant content increased. The magnetic behavior of the materials was studied using vibrating sample magnetometer (VSM). The saturation magnetization values and magnetic coercivity values decreased with the increase of La^{3+} concentration. The saturation magnetization (M_s) of the ferrite materials decreased with the reduction of size.

1. Introduction

In general, ferrites materials are well known and presented with the molecular formula of AB_2O_4, where the A-site represents the divalent cations and B-site is trivalent cations. The crystallographic study of fcc lattice ferrites is of with Fd3m space group. Oxygen is arranged with 64 tetrahedral at A-site and 32 octahedral interstitial sites at B-site in the unit cell of Polycrystalline spinel ferrite. Metal cations occupied eight of these tetrahedral A-sites and sixteen of octahedral B-sites. In the inverse spinel structure, cations migrate to occupy the vacant interstitial sites of a crystalline structure during the preparation. The electrical, magnetic and optical properties of ferrites are mostly reliant on many factors, as synthesis technique, annealing temperature, chemical compositions, and the occupancy and migration of cations among A-B sites [1]. Due to remarkable properties of Cobalt ferrite such as chemical stability, high coercivity, moderate saturation magnetization, and good mechanical hardness, it has attracted considerable attention [2]. The cobalt ferrite materials are famous due to their large magneto-crystalline anisotropy energy with positive anisotropy constant (K1) which is a classic and distinct aspect of hard magnetic materials [3]. This magneto-crystalline anisotropy constant relies upon the synthesis method along with annealing temperature [4]. The Cobalt ferrite has versatile magnetic properties because it has numerous usages for example in high-density magnetic recording media, magnetic resonance imaging (MRI) contrast agents, electronic engineering, and telecommunication [5-6]. This material has a ability of tuning in magnetic system because of smart replacement of various transition and non-transition elements on A and/or B site. In the recent studies, replacements of trivalent cations at the Fe^{3+} sites in cobalt ferrite, creates the effective modifications in the electric, magnetic and structural properties of the material [7]. Toksha et al. [8] reported that the structural and magnetic properties of cobalt ferrite are remarkably changed by the entity of Cr^{3+} ions. The chromium ions are included in those transition metal ions which always take the position of Fe^{3+} B-site and control the magnetic parameters such as coercivity and remanence. Similarly, other author's reports are available on Cr^{3+} substituted cobalt ferrite

synthesized by different methods [9-11]. It has been reported that variation in magnetic characteristics of cobalt ferrite are due to the leading super-exchange between the cations of A-site and B-site via oxygen ions. Magnetic properties of spinel cobalt ferrite can be the modified results have been reported by replacement of minor amount of rare-earth elements at of Fe^{3+} ions [12]. However, the synthetization of nano-crystalline rare-earth-doped cobalt ferrite materials in a single phase is a difficult task. Many drawbacks are reported in the spinel ferrites structure even for low concentration of Re^{3+} ions such as the phase segregation of ortho-ferrites ($ReFeO_3$) [13-14], hematite (α-Fe_2O_3) [15-16] and metal monoxides [17]. The other problem is to control the crystal size of cobalt ferrite which is due to the high nucleation rate that resists synthesizing the uniform size materials. The substitution of La^{3+} in the crystalline structure of cobalt ferrite has been reported and studied the structural and magnetic properties. Kumar et al. [20] reported that in the spinel ferrites, the saturation magnetization decreases with increases of La^{3+} ions concentration. Kim et al; [18] and Tahar et al; also substituted La^{3+} ions in cobalt ferrites materials and reported that saturation magnetization increases and coercivity decrease with increase of annealing temperature [19]. Burianova et al. [21] reported that the coercivity of material depends on the size of the crystal rather than that of concentration of La^{3+} ion. According to best of our knowledge, very few studies has been reported in the literature, on the study of structure and magnetic properties of Cr^{3+} and La^{3+} substituted cobalt ferrite. The present work aims to study the structural and magnetic properties of La^{3+} substituted $CoCr_{0.04}La_xFe_{1.96-x}O_4$ (where Cr^{3+} = 0.04 and $0.0 \leq x \leq 0.12$) ferrites by using co-precipitation technique.

2. Materials And Methods

2.1. Samples preparation and equipment

Chemical compound such as $Co(NO_3)_2.6H_2O$, $Cr(NO_3)_36H_2O$, $Fe(NO_3)_3.9H_2O$ and $La(NO_3)_36H_2O$ were used in the synthetization of ferrite samples with formula $CoCr_{0.04}La_xFe_{(1.96-x)}O_4$ (x = 0.0- 0.12 with in step 0.02) by the co-precipitation method. These chemical compounds were made into solution using deionized water. The sodium hydroxide (NaOH) was also be used as precipitant. The pH value of the solution was maintained at 11 and it was stirred for 1 hour with the help of magnetic stirrer. The obtained precipitates were digested at 85^oC in the water bath for the duration of 30 minutes. The precipitates were then washed with deionized water. The final product was dried at 95°C in an oven model WHL-25AB. The obtained powder was pelletized under the load of 35 N/cm^2 for 3 min by Paul-Otto Weber Hydraulic Press. In order to remove oxide layer or polishing, each sample of powder and pellet (6 mm x 2 mm) were sintered in a programmable computerized furnace model SNOL at 900°C for six hour. The XRD technique is recommended for the microstructural studies. Therefore, the Xpert Pro PANalytical diffractometer with Cu-Kα radiation (λ = 1.54056 Å) at 40 kV and 30 mA has been used for characterization of each sample. The XRD intensity spectra were recorded with a scanning speed 0.05° /s in the 2θ range from 20-70°. Other important study is surface morphological studies of the samples. These studies were performed using a high quality and vigilant device, named as JSM-6490 JEOL, scanning electron microscope (SEM). The

elemental composition was made to confirm using energy dispersive X-ray spectroscopy (EDXS, Model JFC-1500 JEOL). The FTIR spectroscopy has been employed using Jasco-310 spectrometer. The frequency range of 400-4000 cm^{-1} was used for present studies. For current-voltage (I-V) characteristics, the source meter of model (Keithly-2410) was used. The vibrating sample magnetometer (VSM) of Lake Shore 735was selected for recording the magnetic properties. The obtained spectra of XRD were used to calculate the crystallite size, lattice constants, unit cell volume, and X-ray density by using the following relations [22-23].

$$a = \frac{\lambda}{2Sin\theta}\sqrt{h^2 + k^2 + l^2} \quad (1)$$

$$V_{cell} = a^3 \quad (2)$$

$$D = \frac{k\lambda}{B_{(hkl)}\cos\theta} \quad (3)$$

$$\rho_{X-ray} = \frac{Z\,M}{N_A\,V} \quad (4)$$

Where ‘a’ is lattice constant in Angstrom, the (hkl) represent Miller indices, V is the volume of unit cell, Z shows 8 molecules per unit cell of the spinel structure of ferrites, N_A represents Avogadro’s number (6.02×10^{23} g/mol) and M is the molecular weight of ferrites sample. Scherer’s equation which has been mentioned in 3 is used for calculating the crystallite size (D) nm, λ is X-ray source wavelength and θ is Bragg’s angle.

3. Results And Discussion

3.1 Structural Analysis

Fig. 1 shows the stalk of XRD spectra of present synthesized ferrite samples. For attaining the single phase each sample was sintered at 900^oC for 6 h duration. The specific diffracting peaks are the characteristics planes which have been marked at (111), (220), (222), (400), (422), (511) and (620). The presence of such set of planes confirms the cubic spinel structure of ferrite. These peaks were indexed through Jade 5 software. Two samples (x = 0.0 and x = 0.02) confirmed their single phase crystalline spinel structure. The other substitutions showed secondary phases. The secondary phases appeared in other samples on grain boundaries due to high reactivity of Fe^{3+} ions along with La^{3+} ions or due to the limited solubility of RE^{3+} ions into the solid solution of prepared ferrites. The calculating values of lattice constants for all the samples were found in the range of 8.3713Å -8.3832Å.

These variations among lattice parameters can be described on the basis participants in the crystalline structure. The ion radii are the concerned participants. The variation in their radii can create different changes. In the present scenario, the substituted element of La^{3+} (1.03Å) ionic radius is larger in size as that of Fe^{3+} (0.67Å) that’s why an increase in lattice parameter is observed. The maximum lattice constant values obtained for x=0.04 (8.3832 Å). The Table1 is summarizing that lattice constant increases with the increase of the La^{3+} contents. The described characteristic peaks have been used for

calculating the lattic parameters and observed values of all the samples have been enlisted in the Table1. The crystallite size of $CoCr_{0.04}La_xFe_{(1.96-x)}O_4$ ferrite samples were estimated using the Debye-Scherer's Eq.3. The obtained crystallite size lies in the range of 53 nm to 106 nm. The in X-ray density increases as La^{3+} -substituting contents is increased which is due to the larger molar mass of La^{3+} (140.3 g/mol) as compared to that for Fe^{3+} (55.84 g/mol). The obtained values of X-ray density lies in the range of 5.31 g/cm^3-5.53 g/cm^3. It may also be attributed being of the pores which can be developed during the sample growth or can exist during sintering process.

Table 1. Lattice constant, Crystallite size (nm), Unit cell volume and X-ray density $CoCr_{0.04}La_xFe_{1.96-x}O_4$ where x= 0 - 012 ferrites

Composition	Lattice Constant (Å)	Crystallite Size (nm)	Unit Cell Volume (Å^3)	X-ray density g/cm^3
$CoCr_{0.04}Fe_{1.96}O_4$	8.3717	67.2	586.73	5.31
$CoCr_{0.04}La_{0.02}Fe_{1.94}O_4$	8.3735	84.8	587.11	5.34
$CoCr_{0.04}La_{0.04}Fe_{1.92}O_4$	8.3832	73.2	589.15	5.36
$CoCr_{0.04}La_{0.06}Fe_{1.90}O_4$	8.3713	62	586.66	5.42
$CoCr_{0.04}La_{0.08}Fe_{1.88}O_4$	8.3619	53	584.69	5.48
$CoCr_{0.04}La_{0.1}Fe_{1.86}O_4$	8.3622	106	584.74	5.52
$CoCr_{0.04}La_{0.12}Fe_{1.84}O_4$	8.3758	84.8	587.59	5.53

3.2 Morphology and Elemental Analysis

The SEM micrographs of samples x=0.0 - 0.08 are given in the Fig.2 (a-d). The grains were like spherical with non-uniform sizes over a particular scanned area. The calculated size of crystallite with Scherrer's formula is used to confirm through the support of SEM device. The micrographs of SEM clarify the size and shape.

From these micrograph it can be seen clearly that appearance of agglomeration may be attributed due to long sintering which produced localized chemical reaction [24] or may be due to the weak van der Waals bonds. The role of La^{3+} ion substitution is to reduce the agglomeration phenomenon in the materials [25-26].

Fig.3 (a-f) shows the spectra of energy dispersive of the ferrites sample with La^{3+} content (a) x = 0.00, (b) x = 0.02, (c) x = 0.04, (d) x = 0.06, (e) x = 0.08 and (f) x = 0.1 which was sintered at temperatures 900°C for 6 h. The experiential EDX results clarify the atomic percentages of Co, La Fe, and O elements which are present in the synthesized nanoparticles (NPs). Each recoded and calculated sample has been presented in the Table 2. These results graded that all samples were pure and had exact compatibility with required constituents of the composition.

Table 2: The elemental composition of $CoCr_{0.04}La_xFe_{1.96-x}O_4$ ferrites

Elements	X= 0.00	X= 0.02	X = 0.04	X = 0.06	X = 0.08	X = 0.1
C (weight %)	7.40	4.50	5.27	3.24	16.21	11.03
O(weight %)	51.08	46.60	56.42	48.88	55.91	29.26
Cr (weight %)	1.03	0.74	0.40	0.71	0.59	1.57
Fe (weight %)	22.83	29.58	20.96	28.53	13.96	34.40
Co(weight %)	11.85	15.65	11.04	15.64	7.35	18.99
La(weight %)	0.00	0.52	0.50	0.99	0.80	1.55

3.3 FTIR Spectroscopy

Fig. 4(a-f) shows the FTIR spectra of La^{3+} substituted Co-Cr- ferrites samples which have been recorded of 400 cm^{-1} - 4000 cm^{-1}. The common investigated features of ferrite spectra show absorption peaks at below 1000 cm^{-1} that represent metal oxygen (M-O) vibration mode [27]. In FTIR results, there are two prominent observed peaks at tetrahedral sites. The high frequency peaks appear in the frequency range 600 cm^{-1} - 500 cm^{-1} due to metal-oxygen stretching. The low frequency peaks in the range 430 cm^{-1} -385 cm^{-1} are corresponding to the appearances of the octahedral sites.

3.4. Current-Voltage Characterization

Fig 5 shows family of current-voltage (I-V) curves for different La^{3+} concentration. The electric resistivity of synthesized samples has been measured by using relation:

$R = \rho L/A$ (5)

where A is the area of pellet, L is width and R is resistance of pellet. The measured electrical resistivity (ρ) of all the synthesized materials with different La^{3+} content depends on the crystalline nature and composition of the material. In the present situation as the La contents are increased this resulted in the increment of resistivity that was in accord with results of Kumar et al [20]. Such behavioral response about resistivity in ferrites materials confirms that they can be applied in high frequency devices.

3.5 Magnetic Properties

In the present work Fig.6 exhibits magnetic hysteresis loops of samples (x = 0.02 and x = 0.04) at room temperature respectively. They show their ferrimagnetic nature through the phenomena of unique saturation magnetization and coercivity. It has become a general perception that magnetic properties of nanoparticles depend on the synthesizing routes along with some specific conditions such as their particle size and distributions of cations on different sites. Saturation magnetization of pure bulk sample cobalt ferrites has been reported Ms (80 emu/g) by [27]. In the present scenario, the effect of tenability

has been controlled through the addition of trivalent cations in the magnetic material. The obtained results are promising because such addition/substitution played a vital role in spin canting at the surface of nanoparticles and moderates overall magnetization. There exist electron couplings due to La^{3+} -Fe^{3+} interaction and the La^{3+}- La^{3+} interaction but they are very weak [28]. In spinel phased ferrites, the saturation magnetization (Ms) becomes dominant with the super-exchange interactions between the tetrahedral and octahedral sites cations. The La^{3+} ions do not play a part in exchanging their positions with nearest neighboring ions. It may be due to their non-magnetic attitude. They have zero magnetic moment due to which number of magnetic linkages starts decreasing. Hence as we increase the La^{3+} concentration, the super-exchange interactions becomes weaken [29].

The La^{3+} ions have strong spin-orbit coupling and promote the asymmetrical structure of the nanoparticles as they are located at the B sites. Another reason for the improvement in coercivity can be attributed due to nucleation, propagation and pinning-depinning of a domain wall, are strongly linked to the microstructure [30].

4. Conclusions

The spinel ferrites, La^{3+}-substituted $CoCr_{0.04}La_xFe_{(1.96-x)}O_4$ (x = 0.0-0.12) has been successfully synthesized with the use of co-precipitation route. The microstructural studies were performed with conventional technique i.e. XRD. The stability of structure was confirmed by calculating different parameters of the synthesized materials. The average crystallite size was found in the range of (53nm-106 nm) using Scherrer's formula. These sizes have been confirmed with scanning electron microscopic images. The SEM analysis not only inveterate the morphology of the synthesized material but also explain the growth of grain size. The characteristics peaks in the spectra of EDX confirmed the stoichiometric ratio of present synthesized samples. The annealing process at suitable higher temperatures such as 900 ^oC and above is selected on the cation distribution. The magnetic properties are greatly responding of higher temperatures. The magneto- crystalline anisotropy constant decreases with the increase in La^{3+} concentration.

Declarations

Acknowledgements

The author (Ghulam Mustafa) is thankful to Higher Education Commission (HEC) of Pakistan for providing financial support to carry out this work under IRSIP scholarship.

Competing interests

The authors declare that they have no known competing financial interests or personal relationships that could have appeared to influence the work reported in this paper.

References

[1] A. Goldman, Modern Ferrite Technology, second ed., Springer, New York, 2006.

[2] R. Valenzuela, Magnetic Ceramics, Cambridge University Press, 1994.

[3] J. Smit, Ferrites, Wiley, New York, 1959.

[4] L. Kumar, M. Kar, Effect of annealing temperature and preparation condition on magnetic anisotropy in nanocrystalline cobalt ferrite, IEEETrans. Magn. 47 (2011) 3645-3648.

[5] E.C. Snelling, Soft Ferrites: Properties and Applications, second ed.,Butterworths, London, UK, 1988.

[6] J.L. Dormann, D. Fiorani, Magnetic Properties of Fine Particles, North-Holland, Amsterdam, 1992.

[7] L. Kumar, M. Kar, J. Magn. Magn. Mater. 323 (2011) 2042-2048.

[8] B.G. Toksha, S.E. Shirsath, M.L. Mane, S.M. Pantage, S.S. Jadjav, K.M. Jadhav,J. Phys. Chem. C 115 (2011) 20905.

[9] M. Anis-ur- Rehman, A. Abdullah, M. Ansari, Zeb-un-Nisa, M.S. Awan, WorldAcad. Sci., Eng. Technol. 76 (2011) 679.

[10] M. Han, C.R. Vestal, Z.J. Zhang, J. Phys. Chem. B 108 (2004) 583.

[11] S.T. Alone, Sagar E. Shirsath, R.H. Kadam, K.M. Jadhav, J. Alloys Compd. 509(2011) 5055.

[12] B.D. Culity, Introduction to Magnetic Materials, Addision-Wesely, 1972.

[13] N. Rezlescu, E. Rezlescu, C. Pasnicu, M.L. Craus, J. Phys.: Condens Matter,6 (1994) 5707-5712.

[14] K.K. Bharathi, J.A. Chelvane, G. Markandeyulu,J. Magn. Magn. Mater. 321(2009) 3677-3680.

[15] E.E. Sileo, R. Rotelo, S.E. Jacobo, Physica B 320 (2002) 257-260.

[16] S.E. Jacobo, W.G. Fano, A.C. Razzitte, Physica B 320 (2002) 261-263.

[17] E.E. Sileo, S.E. Jacobo, Physica B 354 (2004) 241-245.

[18] W.C. Kim, S.J. Kim, J.C. Sur, C.S.Kim, J.Magn.Magn. Mater.242 (2002) 197-200.

[19] L.B. Tahar, M. Artus, S. Ammar, L.S. Smiri, F. Herbst, M.J. Vaulay, V.Richard, J.M.Greneche, F.Villian, F. Fievet, J. Magn. Magn. Mater. 320 (2008) 3242-3250.

[20] P. Kumar, S.K.Sharma, M. Knobel, M.Singh,J.Alloy.Compd.508 (2010) 115-118.

[21] S. Burianova, J.P. Vejpravova, P. Holec, J. Plocek, D. Niznansky, J. Appl. Phys. 110 (2011), 073902-073907

[22] G. Mustafa, et al., Journal of Magnetism and Magnetic Materials 378, 409 (2015).

[23] G. Mustafa, et al., Journal of Magnetism and Magnetic Materials 387, 147 (2015).

[24] A.Goldman,Modern Ferrite Technology,2nd ed.,Springer Publication,(2006) 83-135

[25] J. Feng, Li-Qin Guo, X. Xu, S.Y. Qi, Mi-Lin Zhang, PhysicaB: Condensed Matter, 394 (2007) 100-103.

[26] J. Wang, C. Zeng, Z.M. Peng, Q.W. Chen, Condensed Matter, 349 (2004) 124-128.

[27] T. George, A.T. Sunny, T. Varghese, IOP Conference Series: Materials Science and Engineering, 73 (2015) 012050.

[28] I. Ali, M. Islam, M. Ishaque, H.M. Khan, M.N. Ashiq, M. Rana, Journal of Magnetism and Magnetic Materials, 324 (2012) 3773-3777.

[29] M.A. John Jacob, Khadar, J. Appl. Phys. 107 (2010) 114310-114320.

[30] F.X. Cheng, J.T. Jia, Z.G. Xu, B. Zhou, C.S. Liao, C.H. Yan, L.Y. Chen, H.B. Zhao, Journal of applied physics, 86 (1999) 2727-2732.

Figures

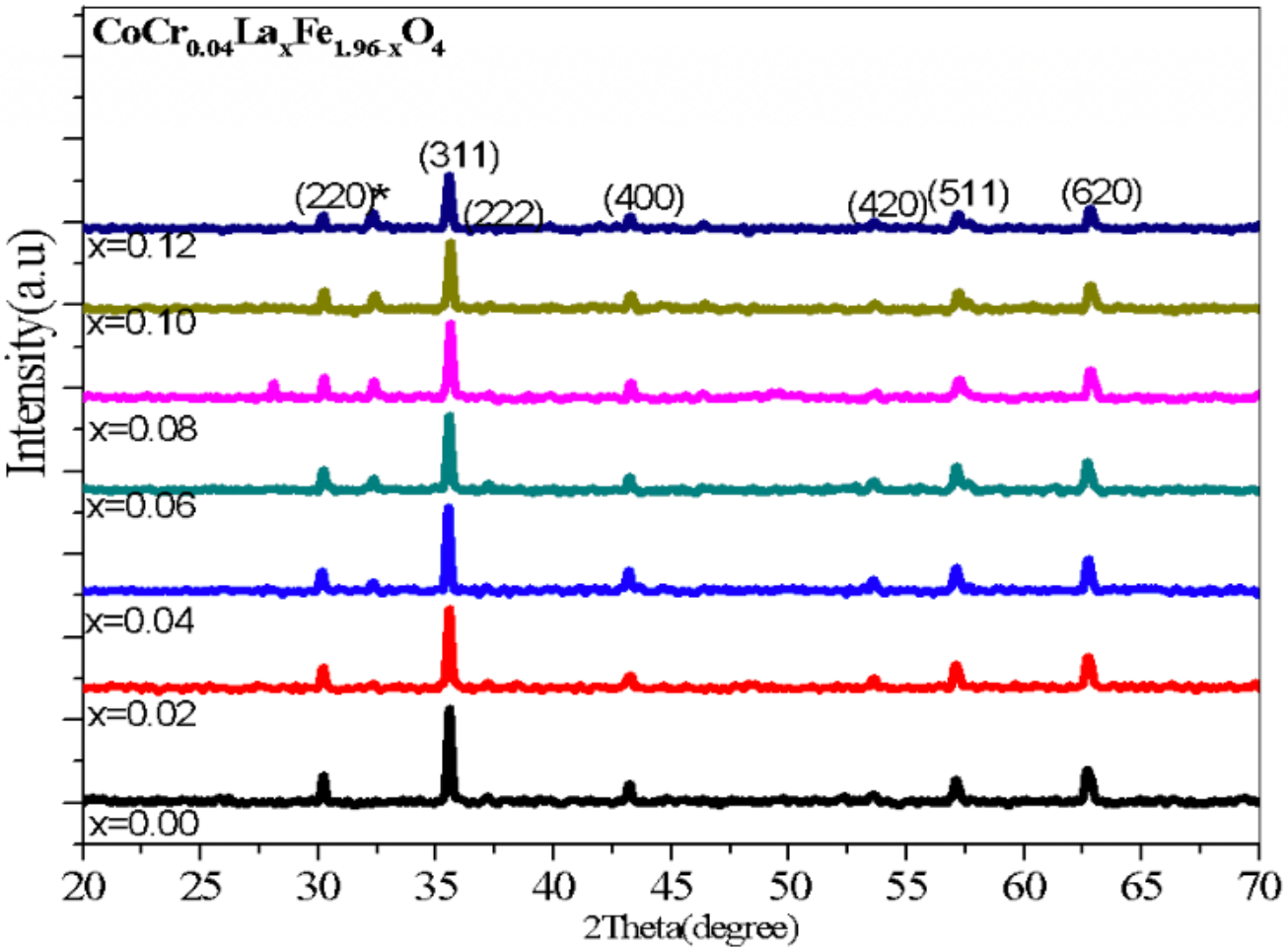

Figure 1

XRD Patterns of CoCr0.04LaxFe1.96-xO4 spinel ferrites

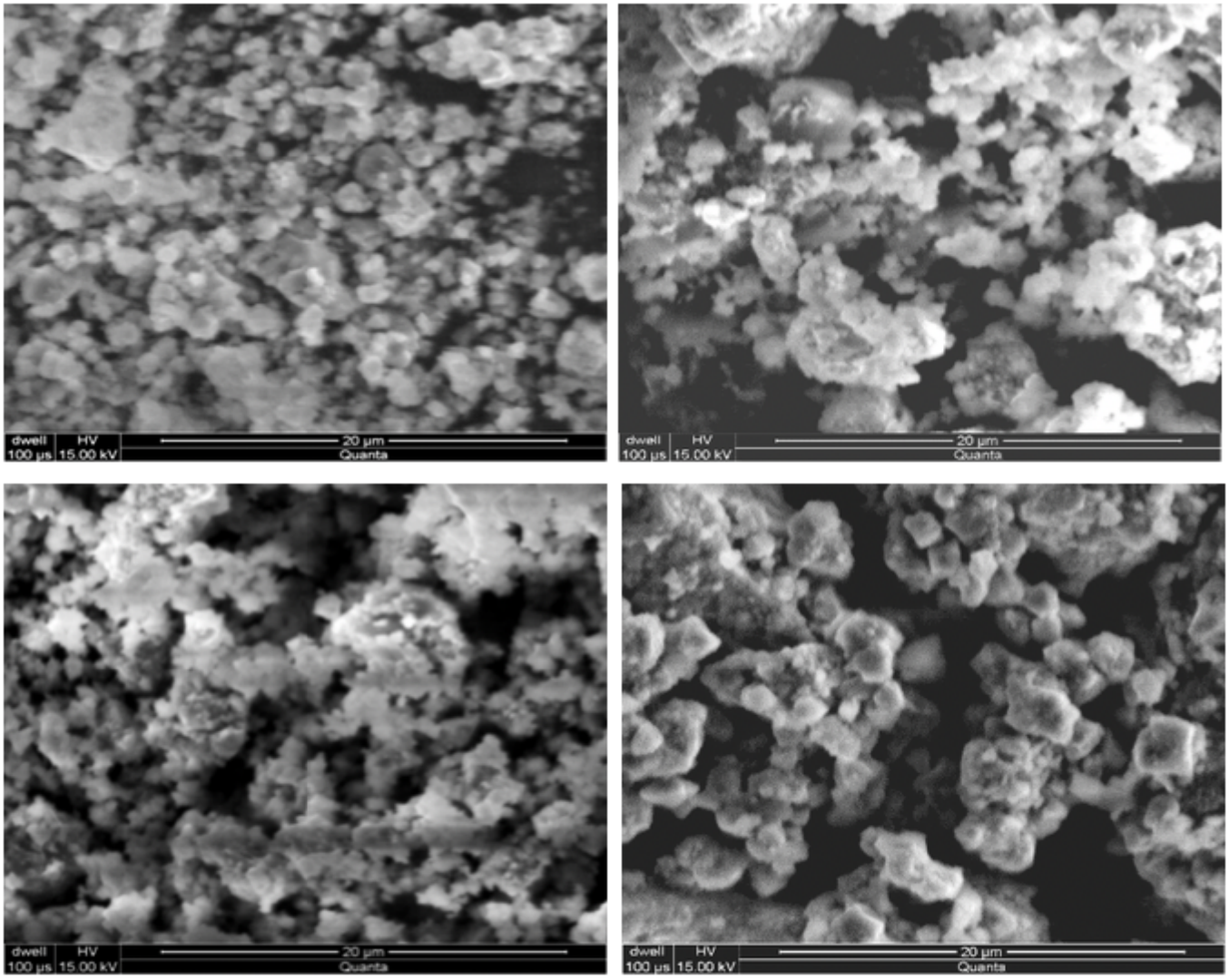

Figure 2

SEM micrographs ofCo-Cr0.04LaxFe1.96-xO4 ferrites (a) x = 0, (b) x = 0.04, (c) x = 0.06 and (d) x = 0.08

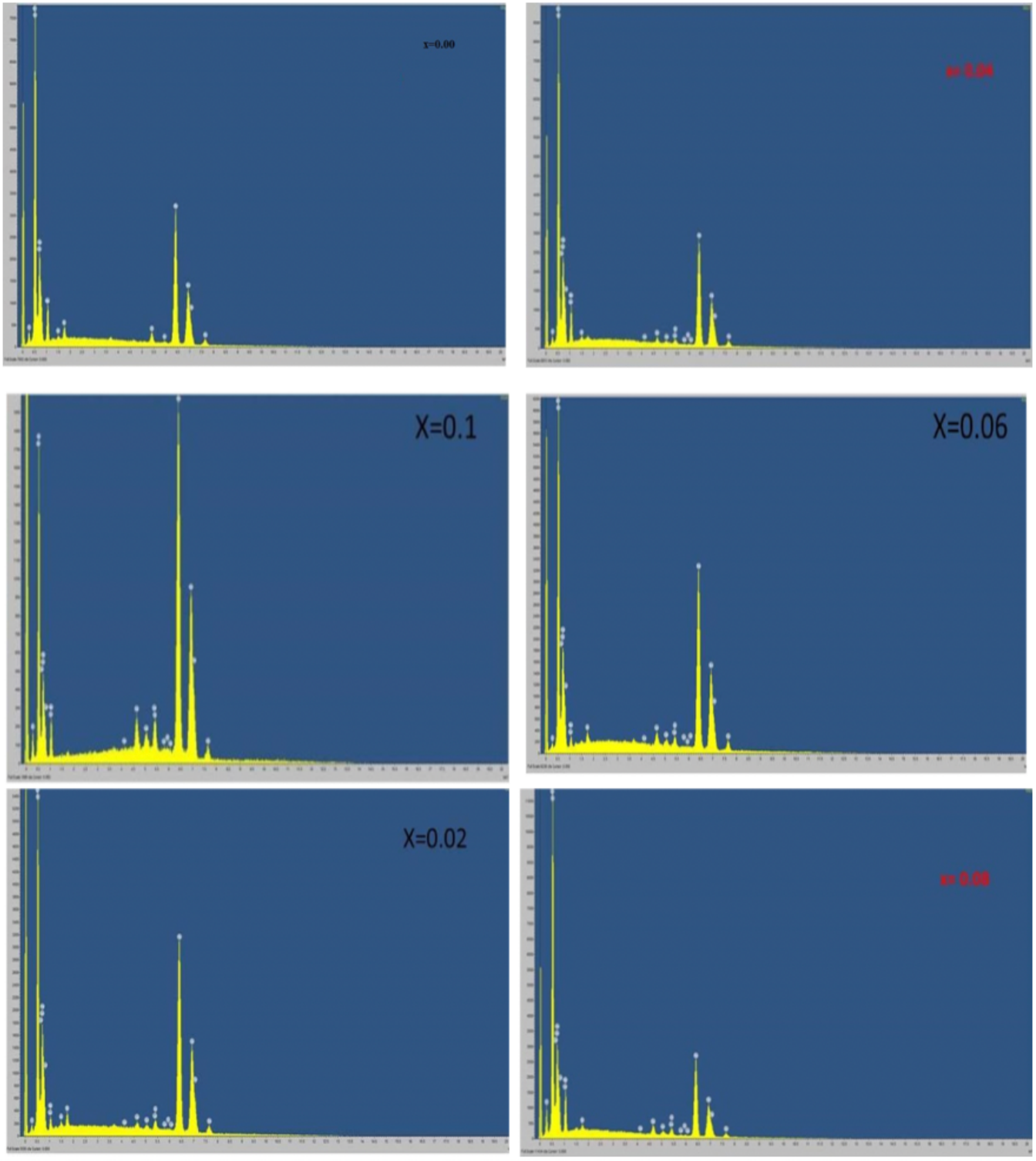

Figure 3

EDX Spectrum for CoCr0.04LaxFe1.96-xO4 ferrites (a) x = 0.00, (b) x = 0.02, (c) x = 0.04, (d) x = 0.06, (e) x = 0.08 and (f) x = 0.1

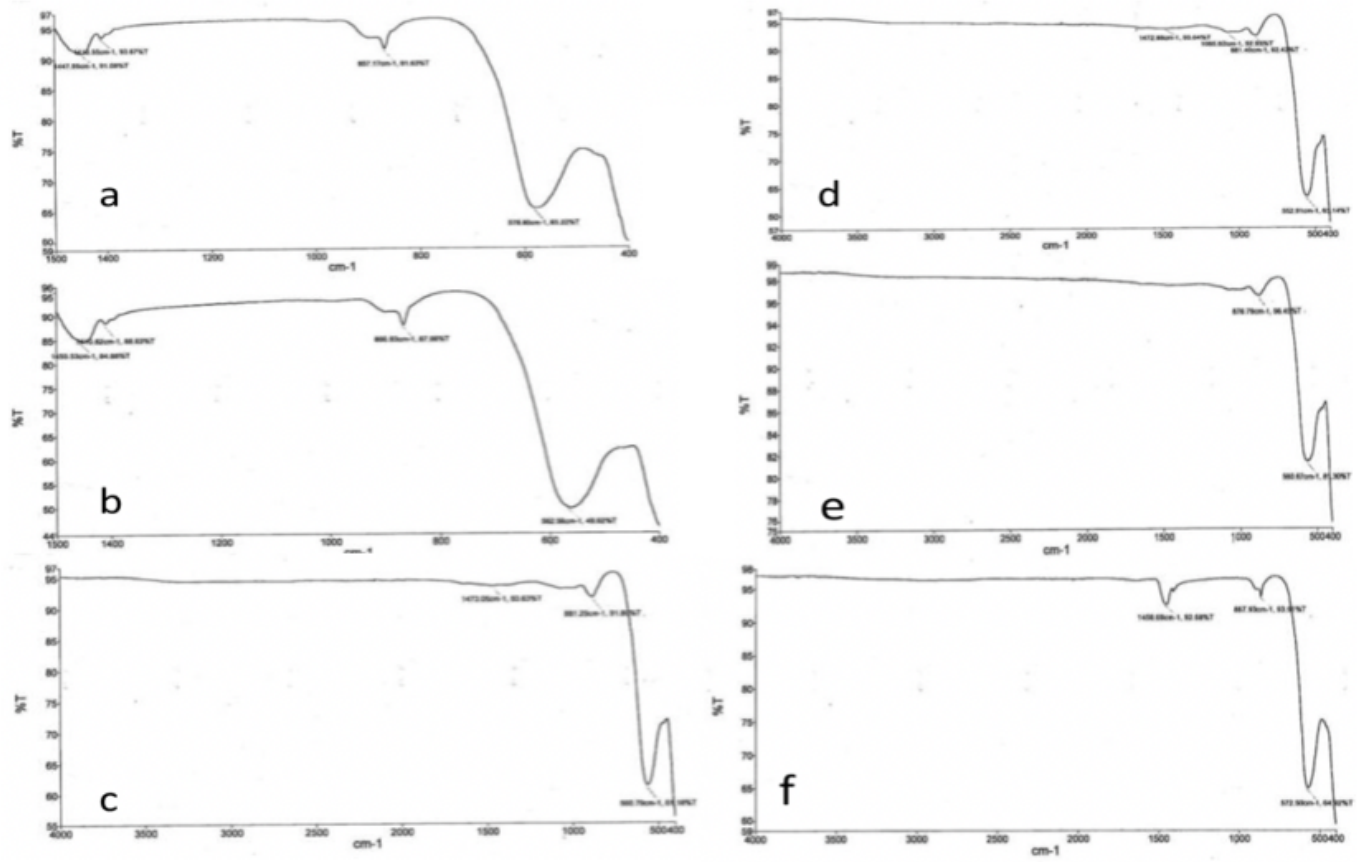

Figure 4

FITR pattern CoCr0.04LaxFe1.96-xO4 ferrites (a) x = 0.00,(b) x = 0.02, (c) x = 0.04, (d) x = 0.06, (e) x = 0.08 and (f) x = 0.1

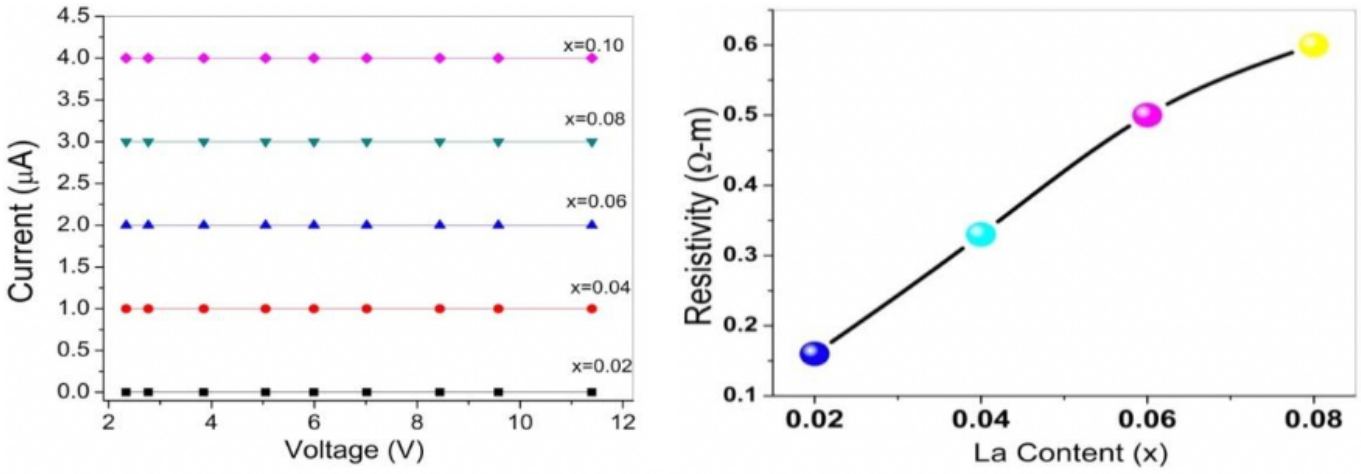

Figure 5

(a) I-V characteristics (b) Resistivity and La3+ content variation of the Co-Cr- ferrites

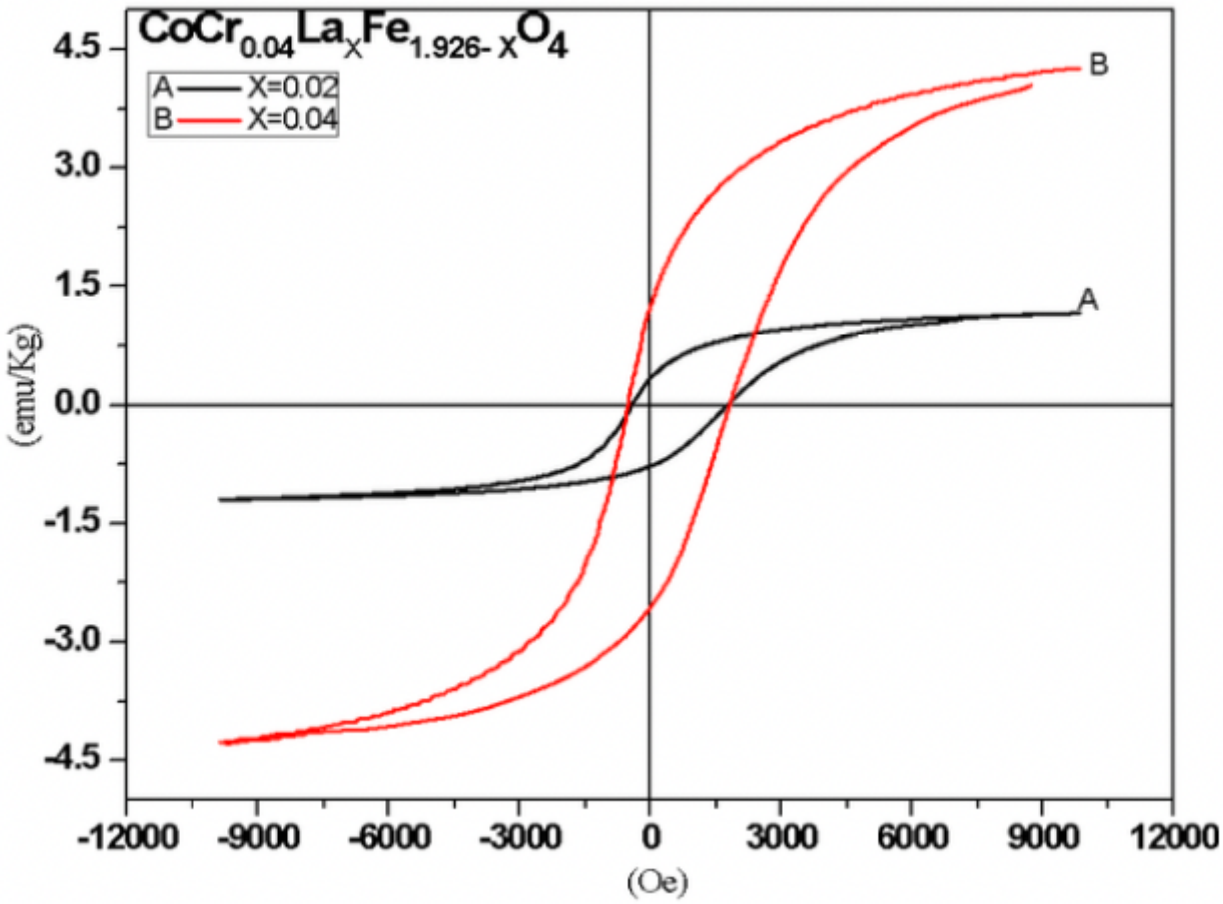

Figure 6

M-H loops of La3+ substituted Co-Cr ferrites at an applied field of 8kOe